Disturbed Ca^{2+} kinetics in *N*-deacetylase/*N*-sulfotransferase-1 defective myotubes

Guido J. Jenniskens[1,*], Maria Ringvall[2], Werner J. H. Koopman[3], Johan Ledin[2], Lena Kjellén[2], Peter H. G. M. Willems[3], Erik Forsberg[2], Jacques H. Veerkamp[1] and Toin H. van Kuppevelt[1,‡]

[1]Department of Biochemistry 194, University Medical Center, NCMLS, 6500 HB Nijmegen, The Netherlands
[2]Department of Medical Biochemistry and Microbiology, Uppsala University, S-751 23 Uppsala, Sweden
[3]Department of Biochemistry 160/Microscopical Imaging Center, University Medical Center, NCMLS, 6500 HB Nijmegen, The Netherlands
*Present address: Biological Engineering Division, Massachusetts Institute of Technology, Cambridge, MA 02139, USA
‡Author for correspondence (e-mail: a.vankuppevelt@ncmls.kun.nl)

Accepted 28 February 2003
Journal of Cell Science 116, 2187-2193 © 2003 The Company of Biologists Ltd
doi:10.1242/jcs.00447

Summary

The biosynthesis of heparan sulfate, present on the cell surface and in the basal lamina surrounding cells, is a multistep process in which each step is mediated by a specific enzyme. The initial modification of the precursor polysaccharide, *N*-deacetylation followed by *N*-sulfation of selected *N*-acetyl-D-glucosamine residues, is catalyzed by the enzyme glucosaminyl *N*-deacetylase/*N*-sulfotransferase (NDST). This event is a key step that regulates the overall sulfate content of the polysaccharide. Here, we report on the effects of NDST deficiency on Ca^{2+} kinetics in myotubes from NDST-1- and NDST-2-deficient mice, indicating a novel role for heparan sulfate in skeletal muscle physiology.

Immunostaining for specific heparan sulfate epitopes showed major changes in the heparan sulfate composition in skeletal muscle tissue derived from NDST-$1^{-/-}$ mice and NDST$^{-/-}$ cultured myotubes. Biochemical analysis indicates a relative decrease in both *N*-sulfation and 2-*O*-sulfation of skeletal muscle heparan sulfate. The core protein of heparan sulfate proteoglycan perlecan was not affected, as judged by immunohistochemistry. Also, acetylcholine receptor clustering and the occurrence of other ion channels involved in excitation-contraction coupling were not altered. In NDST-$2^{-/-}$ mice and heterozygous mice no changes in heparan sulfate composition were observed. Using high-speed UV confocal laser scanning microscopy, aberrant Ca^{2+} kinetics were observed in NDST-$1^{-/-}$ myotubes, but not in NDST-$2^{-/-}$ or heterozygous myotubes. Electrically induced Ca^{2+} spikes had significantly lower amplitudes, and a reduced removal rate of cytosolic Ca^{2+}, indicating the importance of heparan sulfate in muscle Ca^{2+} kinetics.

Key words: Acetylcholine receptor, Ca^{2+}, Heparan sulfate, Sulfotransferase, Skeletal muscle

Introduction

Heparan sulfate proteoglycans (HSPGs) present on the cell surface and in the basal lamina (BL) surrounding cells are involved in various biological processes. The HS chains, which are covalently attached to a protein core, exert their biological functioning through the selective binding of proteins. These interactions depend on HS domains with specific patterns of sulfation (Kjellén and Lindahl, 1991; Salmivirta et al., 1996; Lindahl et al., 1998; Bernfield et al., 1999). The complex processes involved in the structural modification of the HS chain that lead to the generation of such domains are beginning to be unraveled. The proposed pathway of HS biosynthesis involves a cascade of enzymes, each responsible for a single modification step (reviewed by Habuchi, 2000; Selleck, 2000; Sugahara and Kitagawa, 2000; Gallagher, 2001).

After formation of a HS precursor polysaccharide, consisting of repeating D-glucuronic acid and *N*-acetyl-D-glucosamine residues, the bifunctional enzyme glucosaminyl *N*-deacetylase/*N*-sulfotransferase (NDST) catalyzes the first modifications of the precursor polysaccharide, where the acetyl group of selected *N*-acetyl-D-glucosamine residues is replaced with a sulfate group. This reaction is a prerequisite for all other modifications such as C-5 epimerization, 2-*O*-sulfation, 3-*O*-sulfation, and 6-*O*-sulfation, which only occur in the vicinity of *N*-sulfate groups (Lindahl et al., 1998).

Four isoforms of NDST have been identified (Hashimoto et al., 1992; Eriksson et al., 1994; Orellana et al, 1994; Aikawa and Esko, 1999). NDST-1 and NDST-2 are widely distributed (Humphries et al., 1997; Humphries et al., 1998; Kusche-Gullberg et al., 1998; Aikawa et al., 2001), whereas NDST-3 and NDST-4 have a more restricted expression. Disruption of the genes encoding NDST-1 (Fan et al., 2000; Ringvall et al., 2000) and NDST-2 (Forsberg et al., 1999; Humphries et al., 1999) gave insights in the roles of these enzymes in the biosynthesis and physiological roles of HS and heparin, a highly sulfated form of HS. NDST-1-deficient mice are capable of synthesizing *N*-sulfated HS, but the sulfate content is significantly lower than that of HS from wild-type mice, indicating the importance of this enzyme in HS biosynthesis (Ringvall et al., 2000). So far, no obvious defects in HS have been found in NDST-2-deficient mice, which instead are unable to synthesize sulfated heparin (Humphries et al., 1999; Forsberg et al., 1999). However, the increased lethality of NDST-1 and NDST-2 double knockout mice, compared to NDST-1-deficient mice, suggests that NDST-2 also plays a role in HS biosynthesis (Forsberg and Kjellén, 2001).

Different roles for HS or heparin in Ca^{2+} kinetics have been suggested, such as the buffering of Ca^{2+} (Bezprozvanny et al., 1993), influencing growth factor signaling (Patel et al., 1998), or regulating the activity of ion channels such as the dihydropyridine receptor (DHPR) (Knaus et al., 1990; Lacinova et al., 1993; Martinez et al., 1996) and the ryanodine receptor (Bezprozvanny et al., 1993; Ritov et al., 1985). The availability of mice deficient in NDST-1 and NDST-2 provides a means to further investigate the role of HS in skeletal muscle Ca^{2+} kinetics in a physiological setting.

In the present study, we report on the effects of the HS deficiency on electrically induced Ca^{2+} spikes. Immunostaining for specific HS epitopes is reduced in skeletal muscle and in cultured myotubes of NDST-$1^{-/-}$, but not in other genotypes. NDST-$1^{-/-}$ myotubes show a significant decrease in the amplitude of Ca^{2+} spikes and a slower removal of cytosolic Ca^{2+}. These results strongly indicate the involvement of HS in skeletal muscle Ca^{2+} kinetics.

Materials and Methods

Materials

All chemicals used were from Merck (Darmstadt, Germany), unless stated otherwise. Anti-perlecan antibody EY90 was a kind gift of Noonan (Istituto Nazionale per la Ricerca sul Cancro, Genova, Italy). Bacterial media (2×TY and LB) and cell culture media were from Life Technologies (Paisley, Scotland), and tissue culture plastics were from Greiner (Frickenhausen, Germany). Bovine serum albumin (fraction V) and NaN_3 were obtained from Sigma (St Louis, MO). Anti-c-*Myc* tag mouse monoclonal IgG (clone 9E10) was from Boehringer Mannheim (Mannheim, Germany), anti-c-*Myc* tag goat polyclonal IgG (A-14), anti-dihydropyridine receptor goat polyclonal IgG (N-19), and anti-ryanodine receptor goat polyclonal IgG (N-19) were from Santa Cruz Biotechnology (Santa Cruz, CA), and anti-pan sodium channel rabbit polyclonal IgG (SP19) was from Alomone (Jerusalem, Israel). Alexa 488-conjugated donkey anti-goat IgG and goat anti-mouse IgG, Alexa 594-conjugated α-bungarotoxin, Indo-1/AM, and Pluronic F127 were purchased from Molecular Probes (Eugene, OR), and Mowiol (4-88) was from Calbiochem (La Jolla, CA). All experiments were performed at ambient temperature (21°C), unless stated otherwise.

Anti-heparan sulfate antibodies

Preparation of phage display-derived c-Myc-tagged anti-HS antibodies AO4B05, AO4B08, AO4F12, RB4CB9, RB4CD12, RB4EA12, and MPB01 was performed as previously described (Jenniskens et al., 2000). Control antibody MPB01 was randomly picked from phage display 'scFv library #1' (Nissim et al., 1994). This antibody does not recognize HS, or heparin, and is not reactive with any of the cells or tissues tested (muscle, brain, kidney, lung) as judged by ELISA and immunohistochemistry.

Mouse skeletal muscle tissue

Mice heterozygous for NDST-1 and NDST-2 were intercrossed to generate offspring of all genotypes as previously described (Forsberg et al., 1999; Ringvall et al., 2000). Both strains have a mixed C57BL/6 and 129/SvJ/Sv genetic background. The NDST-$1^{-/-}$ mice were obtained from the F4-8 generation, following back-crossing against C57BL/6, while the NDST-$2^{+/-}$ mice were all of the F6 generation. The first day of occurrence of a vaginal plug was taken as day 0 of gestation (E0). E18.5 (18.5 days in utero) embryos were isolated by caesarian delivery and killed by decapitation, in accordance with the ethic regulations of the University. Embryos were rinsed in PBS, snap-frozen in liquid nitrogen-cooled isopentane, and stored at –80°C.

Immunohistochemistry

Cryosections of whole embryos were cut (5 to 10 μm thick), mounted on slides, dried thoroughly, and stored at –80°C until use. Cell cultures were washed three times with PBS, dried overnight, and stored at –80°C until use. Cryosections and cell cultures were stained with anti-heparan sulfate, anti-perlecan, and anti-DHPR antibodies, and with α-bungarotoxin as previously described (Jenniskens et al., 2000). Photographs were taken, using a constant shutter time, on a Zeiss Axioskop immunofluorescence microscope (Göttingen, Germany). For each genotype, skeletal muscle specimens of individual embryos of two separate litters were studied.

Structural analysis of HS from wild-type and NDST-1-deficient muscle tissue

Embryos from a crossing of heterozygous mice (NDST-$1^{+/-}$) were killed and genotyped at embryonic day 18.5. Hind leg muscle tissue was isolated and the samples were lyophilized. The average dry weight was 5.7 mg. HS from the samples was isolated and degraded by enzymatic cleavage, and the disaccharides obtained were separated by reverse phase ion-pair chromotography, followed by labelling with 2-cyanoacetamide, as previously described (Staatz et al., 2001). The obtained disaccharides were separated by reverse phase ion-pair chromatography, followed by labeling with 2-cyanoacetamide. The disaccharides were detected fluorometrically.

Primary myoblast culture

To obtain primary myoblast cultures, E18.5 embryos were isolated by caesarian delivery, killed by decapitation, and dissected (disposed of skin and other organs). Skeletal muscle tissue was isolated from the remaining carcasses, triturated with needles and incubated in an enzyme solution (300 U collagenase/ml, 0.15% trypsin, and 0.08% BSA in PBS, pH 7.3) at 37°C for 15 minutes. To the cell suspension, containing satellite cells (precursors of myoblasts), an equal volume of neutralization solution (DMEM/50% fetal bovine serum [FBS]) was added. The dissociation procedure was repeated three times. Subsequently, cell suspensions were sieved through a 40 μm cell strainer and cells were collected by centrifugation (10 minutes, 50 ***g***). Cell pellets were resuspended and enriched for myoblasts by pre-plating twice for 30 minutes, after which cells were seeded at 5×10^4 cells per well in a six-well format. Primary myoblast cultures were maintained as proliferating cells for up to six passages in DMEM supplemented with 10% brain extract and 1% Ultroser G (Portiér et al., 1999). Cells were plated at 2×10^5 (six-well format) or 5×10^4 (24-well format) cells per well and grown overnight in proliferation medium to reach 50-60% confluency the next day. At confluency, culture medium was replaced by differentiation medium (DMEM/10% brain extract/0.4% Ultroser G). Differentiation medium was refreshed every second day. For immunocytochemistry, H_2SO_4-etched 13 mm diameter coverslips were used in 24-well format. For measurements of cytosolic Ca^{2+}, cells were plated on H_2SO_4-etched 24 mm diameter glass coverslips in six-well format. Cultures were grown and differentiated at 37°C in a humidified 5% CO_2, 95% air atmosphere. For each genotype, primary myoblast cultures derived from at least two individual embryos of two (NDST-2) or three (wildtype and NDST-1) separate litters were studied.

Ratiometric measurements of intracellular Ca^{2+} with Indo-1

Coverslips with confluent monolayers of primary myoblast cultures, differentiated for three days, were washed twice with physiological

salt solution (PSS; 125 mM NaCl, 10 mM $NaHCO_3$, 1 mM NaH_2PO_4, 5 mM KCl, 2 mM $MgSO_4$, 1.8 mM $CaCl_2$, 10 mM HEPES and 10 mM glucose, pH 7.4) and loaded with Indo-1 using an Indo-1/AM solution (5 μM Indo-1/AM and 1 μM Pluronic F127 in PSS) for 45 minutes. Cell loading was performed at 37°C in a humidified 5% CO_2, 95% air atmosphere. Cells were washed twice with PSS, placed in a Leiden chamber (Ince et al., 1985), and incubated in PSS for another 15 minutes. The Leiden chamber was placed on a Nikon diaphot inverted microscope attached to an OZ confocal laser scanning microscope (Noran instruments, Madison, WI). Electrical stimulation of myotubes was performed at 15 to 20 V with 10 milliseconds duration and 0.025 milliseconds delay. Repetitive stimuli were generated at a frequency of 1 Hz. Stimulation was performed using a pair of parallel oriented platinum electrodes (5 mm interspaced, placed beside the monolayer), connected to a Grass SD9 electric pulse generator. Ca^{2+} free medium was obtained by the use of Ca^{2+}-free PSS, supplemented with 1 mM EGTA. For ratiometric Ca^{2+} recordings, Indo-1 was excited at 351 nm using a hardware-modified high power argon-ion laser (Coherent Enterprise, Santa Clara, CA). After being separated by a 455 DCLP dichroic mirror, Indo-1 fluorescence intensity was collected at 405±45 nm and 485±45 nm using photo multipliers. All measurements were performed at room temperature, using a Nikon ×40 water-immersion objective, NA 1.2 with high UV transmission. The estimated laser intensity at the end of the objective lens was 28 μW. Confocality (optical section thickness: 1 to 2 μm) was achieved by using a slit width of 100 μm (Koopman et al., 2001). User-based hardware set-up and data acquisition was controlled by Intervision software (Version 1.5, Noran Instruments), running under IRIX 6.2 on an Indy workstation (Silicon Graphics, Mountain View, CA) equipped with 128 MB of RAM. To improve signal-to-noise ratio, single full-frame images (512×480 pixels) were collected at 30 Hz by averaging of 32 images for each Indo-1 emission wavelength. Pairs of fluorescence intensities were saved in SGI-movie (mv) format, ready for off-line analysis using the Intervision 2D software package (Noran Instruments). Regions of interest (ROI) were drawn and numerical values were stored in ASCII-format. Additional data-analysis was carried out by using Origin 6.0 (Microcal, Northampton, MA), supplemental image analysis and visualization were performed with Image Pro-plus 4.1 (Media Cybernetics, Silver Spring, MD).

Results

Occurrence of HS epitopes in situ in skeletal muscle

We have previously selected antibodies that recognize specific HS epitopes using phage display (van Kuppevelt et al., 1998; Jenniskens et al., 2000). Some of these antibodies were used in this study to investigate the occurrence of various HS epitopes (AO4B05, AO4B08, AOF412, RB4CB9, RB4CD12 and RB4EA12) in intercostal muscle of mouse (E18.5) embryos bearing a targeted disruption of the NDST-1 or the NDST-2 loci (Forsberg et al., 1999; Ringvall et al., 2000). All epitopes studied were present in the BL surrounding muscle fibers and/or nerves of wild-type embryos (Fig. 1a,e) and in embryos heterozygous for NDST-1 and NDST-2 (data not shown). Staining for HS epitopes was significantly reduced in NDST-$1^{-/-}$ muscle BL, except for the neuromuscular region (Fig. 1c) and neural tissue (Fig. 2b). In contrast, NDST-$2^{-/-}$ muscle BL stained normally (Fig. 1g).

When compared to other genotypes, the diameter of myofibers was slightly less uniform in NDST-$1^{-/-}$ muscle, whereas the overall muscle fiber morphology seemed normal. The occurrence and size of neuromuscular junctions (NMJs) were normal, as judged from the staining of acetylcholine receptor clusters. Similarly, staining intensities remained virtually unaltered for other ion channels involved in skeletal muscle excitation-contraction coupling, e.g. the voltage gated sodium channel (data not shown), the DHPR (Fig. 2c,d), and the ryanodine receptor (data not shown). The occurrence and the distribution of the HSPG perlecan core protein was not affected in NDST-$1^{-/-}$ muscle (Fig. 2e,f).

Disaccharide composition of HS from wild-type and NDST-1-deficient muscle tissue

HPLC analysis of fully digested HS, isolated from wild-type and NDST-$1^{-/-}$ skeletal muscle, indicated a decrease in sulfation in NDST-$1^{-/-}$ muscle (Fig. 3). The amount of *N*-

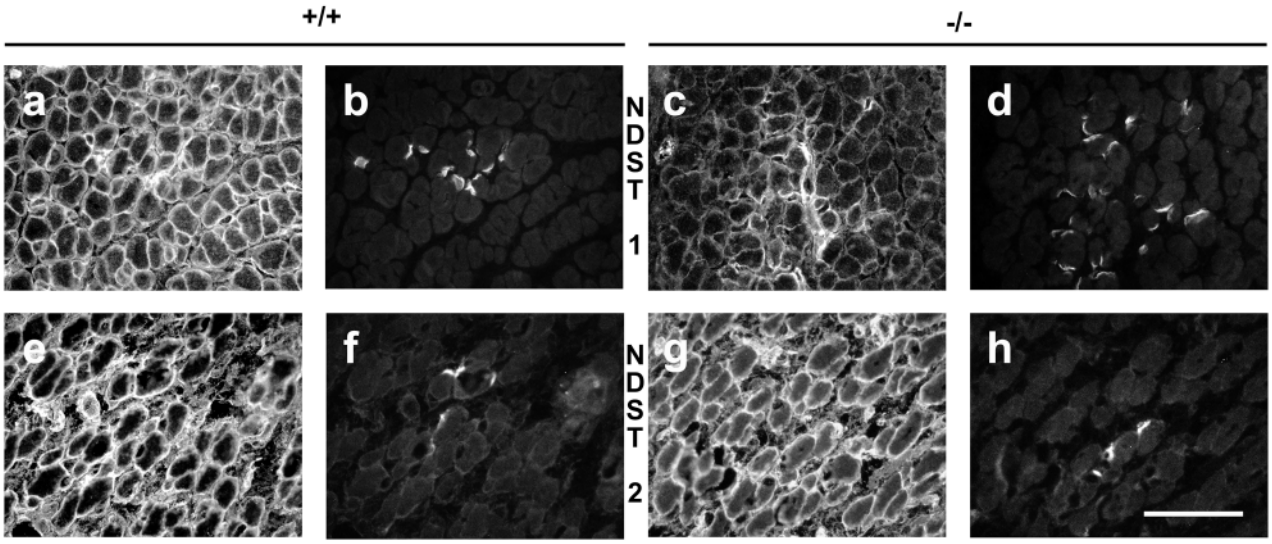

Fig. 1. Reduction of HS epitopes in NDST-$1^{-/-}$ skeletal muscle. Immunofluorescence staining for (a,c,e,g) HS-epitope AO4B05 and (b,d,f,h) acetylcholine receptor clusters in intercostal muscle of E18.5 embryos of (a,b,e,f) wildtype, (c,d) NDST-$1^{-/-}$and (g,h) NDST-$2^{-/-}$. Overall staining in NDST-$1^{-/-}$ is significantly reduced, compared to wild type and NDST-$2^{-/-}$ staining, except for the BL in the NMJs and their direct vicinity (*n*=5; see also Fig. 2a,b). Bar, 50 μm.

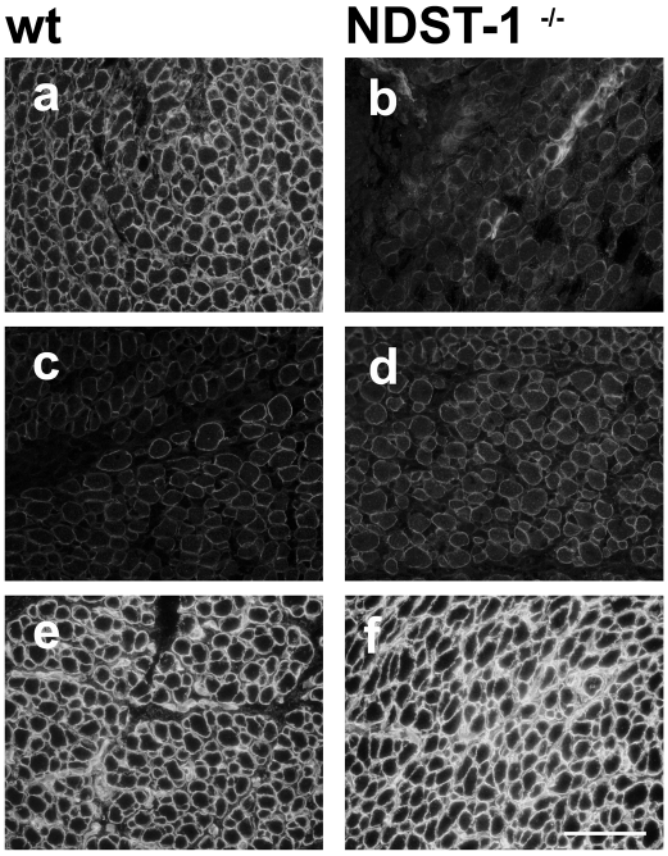

Fig. 2. The distribution of the dihydropyridine receptor (L-type Ca^{2+} channel) and the perlecan core protein are unaffected in NDST-$1^{-/-}$ skeletal muscle. Immunofluorescence staining for (a,b) HS-epitope AO4B05, (c,d) DHPR, and (e,f) perlecan core protein in (a,c,e) wild type and (b,d,f) NDST-$1^{-/-}$ skeletal muscle. Overall staining for HS epitope AO4B05 is significantly reduced in (b) NDST-$1^{-/-}$, compared to (a) wild-type muscle, whereas staining (c,d) for DHPR and (e,f) for perlecan remains virtually unaltered. Note the persistence of staining in neural tissue in (b) (n=3). Bar, 75 μm.

acetylated HS disaccharides was significantly increased and the level of *N*-sulfation was significantly reduced. Also, 2-*O*-sulfation was lower, whereas 6-*O*-sulfation was normal. These results are similar to those obtained in studies of HS from wild-type and NDST-1-deficient liver (J.L., M.R., L.K. et al., unpublished).

Culturing of primary myoblasts

Primary myoblast cultures were generated from muscle tissue of E18.5 embryos. At three days of differentiation, multi-nucleated myotubes were present in all cultures. From day three of differentiation onwards, spontaneous contractions were regularly observed in wild-type and heterozygous myotubes, but only occasionally in knockout myotubes. In wild-type and heterozygous cultures, spontaneous contracting myotubes caused monolayers to peel off from the culture plastics, an effect that was not observed in NDST-$1^{-/-}$ and NDST-$2^{-/-}$ cultures.

Occurrence of HS epitopes in vitro

To analyze the occurrence of HS epitopes in cultured myotubes, three-day-differentiated cultures were stained immunologically. All anti-HS antibodies stained the BL of wild type (Fig. 4a,e) and heterozygous (data not shown) myotubes. Normal BL staining was present in NDST-$2^{-/-}$ cultures (Fig. 4g). However, NDST-$1^{-/-}$ cultures showed hardly any HS staining, even at sites of spontaneous acetylcholine receptor clustering (Fig. 4c), indicating the inability of NDST-1-deficient myotubes to synthesize the HS epitopes recognized by the antibodies.

The clustering of acetylcholine receptors appeared normal in muscle cultures of all genotypes, as judged by α-bungarotoxin staining (Fig. 4, arrows). As was also shown in situ, the in vitro occurrence of the HSPG perlecan core protein was not affected by NDST-1 or NDST-2 deficiency (data not shown).

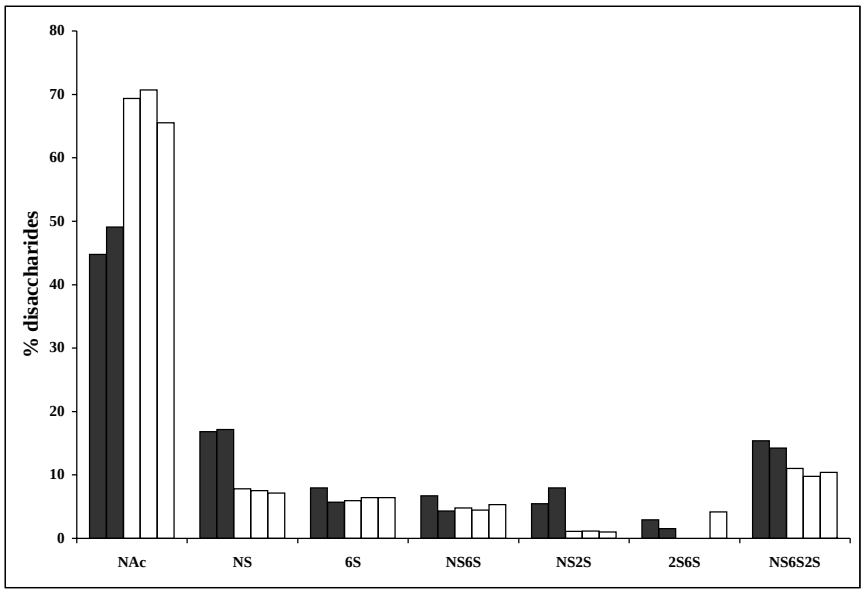

Fig. 3. Alteration of *N*- and *O*-sulfation levels in skeletal muscle of NDST-$1^{-/-}$ mouse. The percentage of *N*-acetylated HS disaccharides (NAc) is strongly increased in skeletal muscle of NDST-$1^{-/-}$ mice (open bars), compared to wild type (solid bars). The *N*-acetylated HS disaccharides fraction may contain a minor portion of chondroitin sulfate. Furthermore, the percentages of *N*-sulfated (NS), *N*-sulfated/2-*O*-sulfated (NS2S), and *N*-sulfated/6-*O*-sulfated/2-*O*-sulfated (NS6S2S) disaccharides are decreased in NDST-$1^{-/-}$ mouse, whereas the percentages of 6-*O*-sulfated (6S), *N*-sulfated/6-*O*-sulfated (NS6S), and 2-*O*-sulfated/6-*O*-sulfated (2S6S) disaccharides are largely unaltered. (Wildtype, n=2; NDST-$1^{-/-}$, n=3).

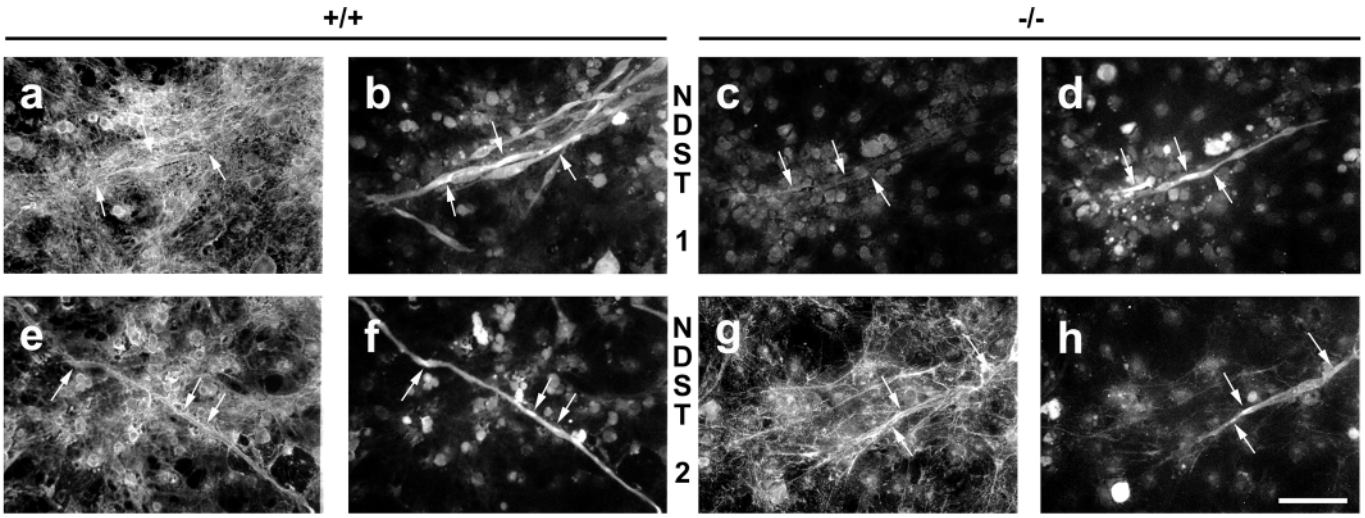

Fig. 4. Reduction of HS epitopes in NDST-$1^{-/-}$ primary muscle cell culture. Immunofluorescence staining for (a,c,e,g) HS-epitope AO4B05 and (b,d,f,h) acetylcholine receptor clusters in (a,b,e,f) wildtype, (c,d) NDST-$1^{-/-}$ and (g,h) NDST-$2^{-/-}$ primary muscle culture after three days of differentiation. HS staining is absent in NDST-$1^{-/-}$derived myotubes and mononuclear cells. In contrast, NDST-$2^{-/-}$ cultures are not affected. Myotubes in all cultures show spontaneous acetylcholine receptors clusters (arrows; *n*=5). Bar, 50 μm.

Electrically induced Ca^{2+} spikes in NDST-1/-2 affected myotubes

Ratiometric measurements of the cytosolic Ca^{2+} concentration ($[Ca^{2+}]_i$) were performed in myotubes of all genotypes, using a high-speed UV confocal laser scanning microscope and electrical stimulation. Average amplitudes of electrically induced Ca^{2+} spikes decreased gradually in the following order: wild type > NDST-$2^{+/-}$ > NDST-$2^{-/-}$ > NDST-$1^{+/-}$ > NDST-$1^{-/-}$, but only NDST-$1^{-/-}$ differed significantly form the wild type (Table 1, Fig. 5). All Ca^{2+} spikes were independent of the presence of Ca^{2+} in the extracellular environment, indicating that the released Ca^{2+} originated from intracellular stores. Upon electrical stimulation, $[Ca^{2+}]_i$ reached its maximum within 99 milliseconds (three data points), after which it rapidly declined to a basal level (Fig. 5), with mono-exponential kinetics ($Y_t=Y_0+Ae^{-t/\mu}$ where Y_t= ratio as a function of time {reflecting the $[Ca^{2+}]_i$}; Y_0= ratio at t=0 {basal ratio, reflecting the basal $[Ca^{2+}]_i$}; A= scaling factor; t= time; μ= decay constant) using the Levenberg-Marquard algorithm (Press et al., 1992). This mono-exponential description was valid because of the small difference between the experimental trace and the fitted exponential function (R^2=0.98) and the small s.e.m. of the average μ (0.26±0.03). The mono-exponential kinetics suggest one main $[Ca^{2+}]_i$ removal process (Koopman et al., 2001; Lieste et al., 1998; de Groof et al., 2002), described by the decay constant μ, which is inversely proportional to the rate of $[Ca^{2+}]_i$ decline

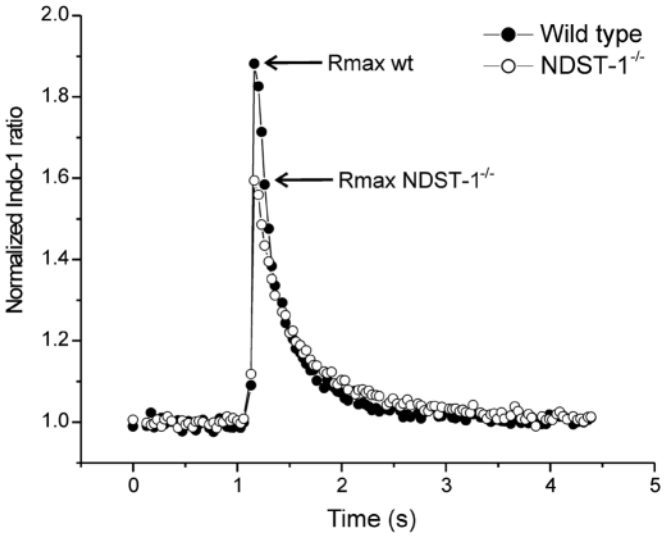

Fig. 5. Disturbed Ca^{2+} kinetics in NDST-1-defective myotubes. Primary myoblast cultures of wild-type and NDST-$1^{-/-}$ embryos were differentiated for three days, and Indo-1 ratios of electrically induced Ca^{2+} spikes were recorded using a high-speed UV confocal laser scanning microscope. Normalized Indo-1 ratios of individual wild-type and NDST-$1^{-/-}$ primary myotubes were averaged and plotted against time, thus generating representative ratio traces for both genotypes. Each point represents the average value (wild type, *n*=12; NDST-$1^{-/-}$, *n*=8).

Table 1. Kinetics of electrically induced calcium spikes in NDST-1/-2 affected myotubes

Genotype	*n**	Amplitude (ratio)‡	Decay constant μ (seconds)‡
Wildtype	12	1.882±0.255	0.264±0.098
NDST-$2^{+/-}$	10	1.872±0.335	0.302±0.142
NDST-$2^{-/-}$	12	1.755±0.242	0.225±0.096
NDST-$1^{+/-}$	13	1.678±0.092	0.319±0.103
NDST-$1^{-/-}$	8	1.594±0.108§	0.426±0.132§

*Analysis was performed on data obtained from myotubes from separate cultures that were derived from individual embryos.

‡Ratiometric measurements of $[Ca^{2+}]_i$ were performed in myotubes of all genotypes, using a high-speed UV confocal laser scanning microscope. Amplitudes and decay constants of electrically induced calcium spikes are given as average values of the number of myotubes analyzed ±s.d.

§P<0.01

(Table 1). NDST-1$^{-/-}$ myotubes differed significantly from wild-type myotubes in decay constant (μ; $P<0.005$). Together with the reduced Rmax this indicates that in these myotubes the quantity of released Ca^{2+} and the $[Ca^{2+}]_i$ removal rate are affected (Table 1; Fig. 5). By plotting μ as a function of Rmax, it was found that the Ca^{2+} removal rate (i.e. $1/\mu$) was positively correlated to Rmax. Only in NDST-1$^{-/-}$ myotubes Ca^{2+} spikes were occasionally skipped upon electrical stimulation, especially when stimulated at high frequency (>1 Hz).

Discussion

Mice deficient in NDST-1 or NDST-2 were used to study the effect of disturbances in HS biosynthesis on excitation-induced Ca^{2+} spiking. Immunostaining of intercostal muscle showed a reduced staining for all HS epitopes studied in the BL of NDST-1$^{-/-}$ mice, except for neuromuscular regions. In NDST-2$^{-/-}$ and heterozygous mice staining was normal. The loss of HS epitopes in NDST-1-deficient muscle indicates a major role for NDST-1 in HS biosynthesis. As previously suggested, NDST-2 appears to be essential for the synthesis of heparin in mast cells but may be marginally involved in HS biosynthesis (Forsberg et al., 1999; Ringvall et al., 2000). All four NDST-isoform transcripts are present in skeletal muscle, NDST-1 and NDST-2 mRNA being more abundant than NDST-3 and NDST-4 transcripts (Aikawa et al., 2001). Studies in liver tissue have shown that there is no transcriptional compensation by other NDST isoforms in NDST-1- and NDST-2-deficient mice (J.L. et al., unpublished) (Grobe et al., 2002). This indicates that other NDST isoforms could have been able to only partially compensate for the loss of NDST-1, resulting in the low levels of sulfation of HS in NDST-1$^{-/-}$ skeletal muscle (Ringvall et al., 2000; Grobe et al., 2002). In particular, the level of *N*-sulfation is reduced in skeletal muscle, as was also observed in studies of fibroblast HS (Ringvall et al., 2000) and liver HS (J.L. et al., unpublished) (Grobe et al., 2002). These results are consistent with the previously reported diminished sulfation levels in NDST-1-deficient cell lines (Bame and Esko, 1989; Ishihara et al., 1993). 2-*O*-sulfation appears to be more affected by the decreased level of *N*-sulfation than 6-*O*-sulfation, most probably because 6-*O*-sulfation also occurs on *N*-acetylated glucosamine residues adjacent to *N*-sulfated ones.

Although staining for HS epitopes was considerably reduced in skeletal muscle from NDST-1$^{-/-}$ mice, the HS content of neural BL and the synaptic BL at the NMJ appeared unaffected, indicating a different HS profile of the latter BLs. Other NDST isoforms may be active in the highly specialized NMJ and neural areas. No obvious effects on the presence of HS epitopes were seen in mice heterozygous for NDST-1, indicating a compensatory effect of the single functional allele present. Also, no effect was observed in NDST-2$^{-/-}$ mice or in mice heterozygous for NDST-2. Overall morphology of NDST-1$^{-/-}$ muscle appeared to be normal, based on immunohistological staining for the ion channels of the excitation-contraction coupling cascade (acetylcholine receptor clusters, voltage gated sodium channels, DHPR, and ryanodine receptor) and for HSPG core protein perlecan, which is present in the BL.

In primary myoblast cultures, staining for HS epitopes in NDST-1$^{-/-}$ cultures was virtually absent, whereas in NDST-2$^{-/-}$ cultures, or in cultures derived from heterozygous mice, staining was normal. The occurrence and size of acetylcholine receptor clusters on myotubes appeared similar in all genotypes, indicating that the loss of either enzyme does not interfere with the proper clustering of this receptor. Also, perlecan core proteins were distributed normally, arguing for a normal protein constitution of the extracellular environment of cultured myotubes.

Ca^{2+} kinetics was affected to various degrees in myotubes of individual cultures. The rate of $[Ca^{2+}]_i$ removal correlated with the amplitudes of Ca^{2+} spikes, both of which were significantly decreased for NDST-1$^{-/-}$ myotubes. The lower amplitude in NDST-1$^{-/-}$ myotubes is indicative of a lowered Ca^{2+} flux over the sarcoplasmic reticulum membrane. Heparin, a highly sulfated HS, binds with high affinity to the extracellular domain of the voltage-dependent L-type Ca^{2+} channel (the DHPR), of skeletal muscle cells (Knaus et al., 1990). Upon stimulation, this receptor induces a conformational change in the Ca^{2+} release channel of the sarcoplasmic reticulum (the ryanodine receptor), resulting in a Ca^{2+} flow from the sarcoplasmic reticulum to the cytosol. HS might be involved in the correct functioning of the dihydropyridine receptor and alterations in HS might reduce the Ca^{2+} flow to the cytosol. Alternatively, the effect of HS could be indirect, e.g. by modulating growth factor signaling. The effect of decorin, a dermatan sulfate proteoglycan, on Ca^{2+} kinetics is mediated through the EGF receptor (Patel et al., 1998). Also, there might be a lowered Ca^{2+} concentration in the sarcoplasmic reticulum (and thus a lowered Ca^{2+} flux) as a result of the NDST-1$^{-/-}$ deficiency. Also, the $[Ca^{2+}]_i$ removal rate is affected in NDST-1$^{-/-}$ myotubes. Since this process is mainly effectuated by sarcoplasmic reticulum Ca^{2+} ATPases, an effect of HS deficiency on the overall Ca^{2+}-pumping rate of this ion pump could be envisioned. The occurrence of skeletal muscle differentiation characteristics such as fusion to multinucleated myotubes, spontaneous acetylcholine receptor clustering, and excitability indicate that myotubes of all genotypes were differentiated to a similarly degree. Therefore, the effects observed are not likely the result of disturbed differentiation.

NDST-1-deficient cultures occasionally failed to generate Ca^{2+} spikes upon electrical stimulation. Such aberrant Ca^{2+} kinetics were not observed in any other genotype, arguing for these effects to be a result of the loss of this enzyme. NDST-1$^{-/-}$ mice die shortly after birth due to respiratory failure. This effect has been attributed to immature type II pneumocytes, resulting in shortage of lung surfactant (Fan et al., 2000; Ringvall et al., 2000). However, the loss of muscle contraction, likely to be the result of disturbed Ca^{2+} kinetics, may also contribute to the lack of pulmonary function.

In this study, we report the effects of the deficiency of NDST-1 or NDST-2 on electrically induced Ca^{2+} spiking in skeletal muscle. The results presented here strongly indicate the involvement of HS in skeletal muscle Ca^{2+} kinetics.

This work was supported by Grant 902-27-184 from the Netherlands Organization for Scientific Research (NWO) and by grants from the Swedish Research Council, Polysackaridforskning AB, the program ‘Glycoconjugates in Biological Systems’, sponsored by the Swedish Foundation for Strategic Research, and Gustaf V:s 80-

årsfond. The authors thank Dr B. van Engelen for constructive discussions.

References

Aikawa, J.-I. and Esko, J. D. (1999). Molecular cloning and expression of a third member of the heparan sulfate/heparin GlcNAc *N*-deacetylase/*N*-sulfotransferase family. *J. Biol. Chem.* **274**, 2690-2695.

Aikawa, J.-I., Grobe, K., Tsujimoto, M. and Esko, J. D. (2001). Multiple isozymes of heparan sulfate/heparin GlcNAc *N*-deacetylase/GlcN *N*-sulfotransferase. Structure and activity of the fourth member, NDST4. *J. Biol. Chem*. **276**, 5876-5882.

Bame, K. J. and Esko, J. D. (1989). Undersulfated heparan sulfate in a Chinese hamster ovary cell mutant defective in heparan sulfate *N*-sulfotransferase. *J. Biol. Chem.* **264**, 8059-8065.

Bernfield, M., Gotte, M., Park, P. W., Reizes, O., Fitzgerald, M. L., Lincecum, J. and Zako, M. (1999). Functions of cell surface heparan sulfate proteoglycans. *Annu. Rev. Biochem.* **68**, 729-777.

Bezprozvanny, I. B., Ondrias, K., Kaftan, E., Stoyanovsky, D. A. and Ehrlich, B. E. (1993). Activation of the calcium release channel (ryanodine receptor) by heparin and other polyanions is calcium dependent. *Mol. Biol. Cell* **4**, 347-352.

de Groof, A. J. C., Fransen, J. A. M., Errington, R. J., Willems, P. H. G. M., Wieringa, B. and Koopman, W. J. H. (2002). The creatine kinase system is essential for optimal refill of the sarcoplasmic reticulum Ca^{2+} store in skeletal muscle. *J. Biol. Chem.* **277**, 5275-5284.

Eriksson, I., Sandbäck, D., Ek, B., Lindahl, U. and Kjellén, L. (1994). cDNA cloning and sequencing of mouse mastocytoma glucosaminyl *N*-deacetylase/*N*-sulfotransferase, an enzyme involved in the biosynthesis of heparin. *J. Biol. Chem.* **269**, 10438-10443.

Fan, G., Xiao, L., Cheng, L., Wang, X., Sun, B. and Hu, G. (2000). Targeted disruption of NDST-1 gene leads to pulmonary hypoplasia and neonatal respiratory distress in mice. *FEBS Letters* **467**, 7-11.

Forsberg, E. and Kjellén, L. (2001). Heparan sulfate: lessons from knockout mice. *J. Clin. Invest.* **108,** 175-180.

Forsberg, E., Pejler, G., Ringvall, M., Lunderius, C., Tomasini-Johansson, B., Kusche-Gullberg, M., Eriksson, I., Ledin, J., Hellman, L. and Kjellén, L. (1999). Abnormal mast cells in mice deficient in a heparin-synthesizing enzyme. *Nature* **400**, 773-776.

Gallagher, J. T. (2001). Heparan sulfate: growth control with a restricted sequence menu. *J. Clin. Invest.* **108**, 357-361.

Grobe, K., Ledin, J., Ringvall, M., Holmborn, K., Forsberg, E., Esko, J. D. and Kjellén, L. (2002). Heparan sulfate and development: differential roles of the *N*-acetylglucosamine *N*-deacetylase/*N*-sulfotransferase isoenzymes. *Biochim. Biophys. Acta* **1573**, 209-215.

Habuchi, O. (2000). Diversity and functions of glycosaminoglycan sulfotransferases. *Biochem. Biophys. Acta* **1474**, 115-127.

Hashimoto, Y., Orellana, A., Gil, G. and Hirschberg, C. B. (1992). Molecular cloning and expression of rat liver N-heparan sulfate sulfotransferase. *J. Biol. Chem.* **267**, 15744-15750.

Humphries, D. E., Lanciotti, J. and Karlinsky, J. B. (1998). cDNA cloning, genomic organization and chromosomal localization of human heparan glucosaminyl *N*-deacetylase/*N*-sulphotransferase-2. *Biochem. J.* **332**, 303-307.

Humphries, D. E., Sullivan, B. M., Aleixo, M. D. and Stow, J. (1997). Localization of human heparan glucosaminyl N-deacetylase/N-sulphotransferase to the trans-Golgi network. *Biochem. J.* **325**, 351-357.

Humphries, D. E., Wong, G. W., Friend, D. S., Gurish, M. F., Qiu, W.-T., Huang, C., Sharpe, A. H. and Stevens, R. L. (1999). Heparin is essential for the storage of specific granule proteases in mast cells. *Nature* **400**, 769-772.

Ince, C., van Dissel, J. T. and Diesselhoff, M. M. (1985). A teflon culture dish for high-magnification microscopy and measurements in single cells. *Pflugers Arch.* **403**, 240-244.

Ishihara, M., Guo, Y., Wei, Z., Yang, Z., Swiedler, S. J., Orellana, A. and Hirschberg, C. B. (1993). Regulation of biosynthesis of the basic fibroblast growth factor binding domains of heparan sulfate by heparan sulfate-*N*-deacetylase/*N*-sulfotransferase expression. *J. Biol. Chem.* **268**, 20091-20095.

Jenniskens, G. J., Oosterhof, A., Brandwijk, R., Veerkamp, J. H. and van Kuppevelt, T. H. (2000). Heparan sulfate heterogeneity in skeletal muscle basal lamina: demonstration by phage display-derived antibodies. *J. Neurosci.* **20**, 4099-4111.

Kjellén, L. and Lindahl, U. (1991). Proteoglycans: structures and interactions. *Annu. Rev. Biochem.* **60**, 443-475.

Knaus, H.-G., Scheffauer, F., Romanin, C., Schindler, H.-G. and Glossmann, H. (1990). Heparin binds with high affinity to voltage-dependent L-type Ca2+ channels. Evidence for an agonistic action. *J. Biol. Chem.* **265**, 11156-11166.

Koopman, W. J. H., Scheenen, W., Errington, R. J., Willems, P., Bindels, R. J. M., Roubos, E. W. and Jenks, B. G. (2001). Membrane-initiated Ca(2+) signals are reshaped during propagation to subcellular regions. *Biophys. J.* **81**, 57-65.

Kusche-Gullberg, M., Eriksson, I., Sandbäck Pikas, D. and Kjellén, L. (1998). Identification and expression in mouse of two heparan sulfate glucosaminyl *N*-deacetylase/*N*-sulfotransferase genes. *J. Biol. Chem.* **273**, 11902-11907.

Lacinova, L., Cleemann, L. and Morad, M. (1993). Ca^{2+} channel modulating effects of heparin in mammalian cardiac myocytes. *J. Physiol.* **465**, 181-201.

Lieste, J. R., Koopman, W. J., Reynen, V. C., Scheenen, W. J., Jenks, B. G. and Roubos, E. W. (1998). Action currents generate stepwise intracellular Ca^{2+} patterns in a neuroendocrine cell. *J. Biol. Chem*. **273**, 25686-25694.

Lindahl, U., Kusche-Gullberg, M. and Kjellen, L. (1998). Regulated diversity of heparan sulfate. *J. Biol. Chem.* **276**, 24979-24982.

Martinez, M., Garcia, M. C., Farias, J. M., Cruzblanca, H. and Sanchez, J. A. (1996). Modulation of Ca^{2+} channels, charge movement and Ca^{2+} transients by heparin in frog skeletal muscle fibres. *J. Musc. Res. Cell Motil.* **17**, 575-594.

Nissim, A., Hoogenboom, H. R., Tomlinson, I. M., Flynn, G., Midgley, C., Lane, D. and Winter, G. (1994). Antibody fragments from a 'single pot' phage display library as immunochemical reagents. *EMBO J.* **13**, 692-698.

Orellana, A., Hirschberg, C. B., Wei, Z., Swiedler, S. J. and Ishihara, M. (1994). Molecular cloning and expression of a glycosaminoglycan *N*-acetylglucosaminyl *N*-deacetylase/*N*-sulfotransferase from a heparin-producing cell line. *J. Biol. Chem.* **269**, 2270-2276.

Patel, S., Santra, M., McQuillan, D. J., Iozzo, R. V. and Thomas, A. P. (1998). Decorin activates the epidermal growth factor receptor and elevates cytosolic Ca2+ in A431 carcinoma cells. *J. Biol. Chem*. **273**, 3121-3124.

Portiér, G. L., Benders, A. A. G. M., Oosterhof, A., Veerkamp, J. H. and van Kuppevelt, T. H. (1999). Differentiation markers of mouse C2C12 and rat L6 myogenic cell lines and the effect of the differentiation medium. *In Vitro Cell. Dev. Biol. Anim.* **35**, 219-227.

Press, W. H., Flannery, B. P., Teukolsky, S. A. and Vetterling, W. T. (1992). *Numerical Recipies in Pascal: The Art of Scientific Computing*. Cambridge, UK: Cambridge University Press.

Ringvall, M., Ledin, J., Holmborn, K., van Kuppevelt, T., Ellin, F., Erikson, I., Olofsson, A.-M., Kjellén, L. and Forsberg, E. (2000). Defective heparan sulfate biosynthesis and neonatal lethality in mice lacking *N*-deacetylase/*N*-sulfotransferase-1. *J. Biol. Chem.* **275**, 25926-25930.

Ritov, V. B., Men'shikova, E. V. and Kozlov, Y. P. (1985). Heparin induces Ca2+ release from the terminal cisterns of skeletal muscle sarcoplasmic reticulum. *FEBS Lett.* **188**, 77-80.

Salmivirta, M., Lidholt, K. and Lindahl, U. (1996). Heparan sulfate: a piece of information. *FASEB J.* **10**, 1270-1279.

Selleck, S. B. (2000). Proteoglycans and pattern formation: sugar biochemistry meets developmental genetics. *Trends Genet.* **16**, 206-221.

Staatz, W. D., Toyoda, H., Kinoshit-Toyoda, A., Chhor, K. and Selleck, S. B. (2001). Analysis of proteoglycans and glycosaminoglycans from Drosophila. *Methods Mol. Biol*. **171**, 41-52.

Sugahara, K. and Kitagawa, H. (2000). Recent advances in the study of the biosynthesis and functions of sulfated glycosaminoglycans. *Curr. Opin. Struct. Biol*. **10**, 518-527.

van Kuppevelt, T. H., Dennissen, M. A. B. A., van Venrooij, W. J., Hoet, R. M. A. and Veerkamp, J. H. (1998). Generation and application of type-specific anti-heparan sulfate antibodies using phage display technology. *J. Biol. Chem*., **273**, 12960-12966.